A Systematic Study of the Photophysical Processes in Polydentate Triphenylene-Functionalized Eu^{3+}, Tb^{3+}, Nd^{3+}, Yb^{3+}, and Er^{3+} Complexes

Stephen I. Klink, Lennart Grave, David N. Reinhoudt, and Frank C. J. M. van Veggel*

Laboratory of Supramolecular Chemistry and Technology and MESA+ Research Institute, University of Twente, P.O. Box 217, 7500 AE Enschede, The Netherlands

Martinus H. V. Werts

Laboratory of Organic Chemistry, University of Amsterdam, Nieuwe Achtergracht 129, 1018 WS Amsterdam, The Netherlands

Frank A. J. Geurts

Department RGL, Akzo Nobel Central Research, P.O. Box 9300, 6800 SB Arnhem, The Netherlands

Johannes W. Hofstraat

Department of Polymers and Organic Chemistry, Philips Research, Prof. Holstlaan 4, 5656 AA Eindhoven, The Netherlands

Received: December 7, 1999; In Final Form: March 3, 2000

m-Terphenyl-based lanthanide complexes functionalized with a triphenylene antenna chromophore ((Ln)**1**) exhibit sensitized visible and near-infrared emission upon photoexcitation of the triphenylene antenna at 310 nm. Luminescence lifetime measurements of the (Eu)**1** and (Tb)**1** complexes in methanol-h_1 and methanol-d_1 revealed that one methanol molecule is coordinated to the lanthanide ion, indicating that all eight donor atoms provided by the ligand are involved in the encapsulation of the lanthanide ion. The luminescence lifetimes of the near-IR-emitting complexes (Er)**1**, (Nd)**1**, and (Yb)**1** in DMSO-h_6 and DMSO-d_6 are in the microsecond range, and are dominated by nonradiative deactivation of the luminescent state. The processes preceding the lanthanide luminescence in the sensitization process have been studied in detail. The complexed lanthanide ion reduces the antenna fluorescence and increases the intersystem crossing rate via an external heavy atom effect. The subsequent energy-transfer process was found to take place via the antenna triplet state in all complexes. Luminescence quantum yield measurements and transient absorption spectroscopy indicated that in solution two conformational isomers of the complexes exist: one in which no energy transfer takes place, and one in which the energy transfer does take place, resulting in the lanthanide luminescence. The intramolecular energy-transfer rate is higher in the (Eu)**1** and (Tb)**1** complexes than in the near-infrared-emitting complexes. In methanol the energy-transfer rate is $3.8 \times 10^7\ s^{-1}$ for (Eu)**1** and (Tb)**1**. In DMSO-d_6 the intramolecular energy-transfer rate is higher in the (Nd)**1** complex ($1.3 \times 10^7\ s^{-1}$) than in the (Er)**1** ($3.8 \times 10^6\ s^{-1}$) and (Yb)**1** ($4.9 \times 10^6\ s^{-1}$) complexes.

Introduction

The excitation of lanthanide ions by energy transfer from an organic antenna chromophore to obtain visible and near-infrared luminescence remains an intriguing concept that can be applied in many areas varying from fluoroimmunoassays[1] to optical signal amplification.[2,3] Provided that most of the excitation energy is transferred from the antenna chromophore to the luminescent lanthanide ion, this process is much more effective than direct excitation, since the absorption coefficients of organic chromophores are many orders of magnitude larger (typically 3−5) than the intrinsically low molar absorption coefficients of trivalent lanthanide ions.[4] The lanthanide luminescence arises from intra-4f transitions which are parity forbidden. As a consequence, the molar absorption coefficients are low (typically 1−10 $M^{-1}cm^{-1}$), and the luminescence lifetimes are relatively long (ranging from microseconds to milliseconds). Moreover, since the 4f orbitals are shielded from the environment by an outer shell of 5s and 5p orbitals, the emission bands remain narrow, even in solution or in an organic matrix at room temperature.

The sensitization pathway in luminescent lanthanide complexes generally consists of excitation of the antenna chromophore into its singlet excited state, subsequent intersystem crossing of the antenna to its triplet state, and energy transfer from the triplet to the lanthanide ion.[5−8] This simple, yet adequate, photophysical model is depicted in Figure 1 together with the lanthanide 4f energy levels responsible for the luminescence. The overall quantum yield of sensitized emission (ϕ_{se}) is therefore the product of the triplet quantum yield (ϕ_{isc}), the energy-transfer quantum yield (ϕ_{et}), and the intrinsic luminescence quantum yield of the lanthanide ion (ϕ_{lum}), hence

* To whom correspondence should be addressed. Fax: +31-53-4894645. E-mail: F.C.J.M.vanVeggel@ct.utwente.nl.

10.1021/jp994286+ CCC: $19.00
Published on Web 05/23/2000

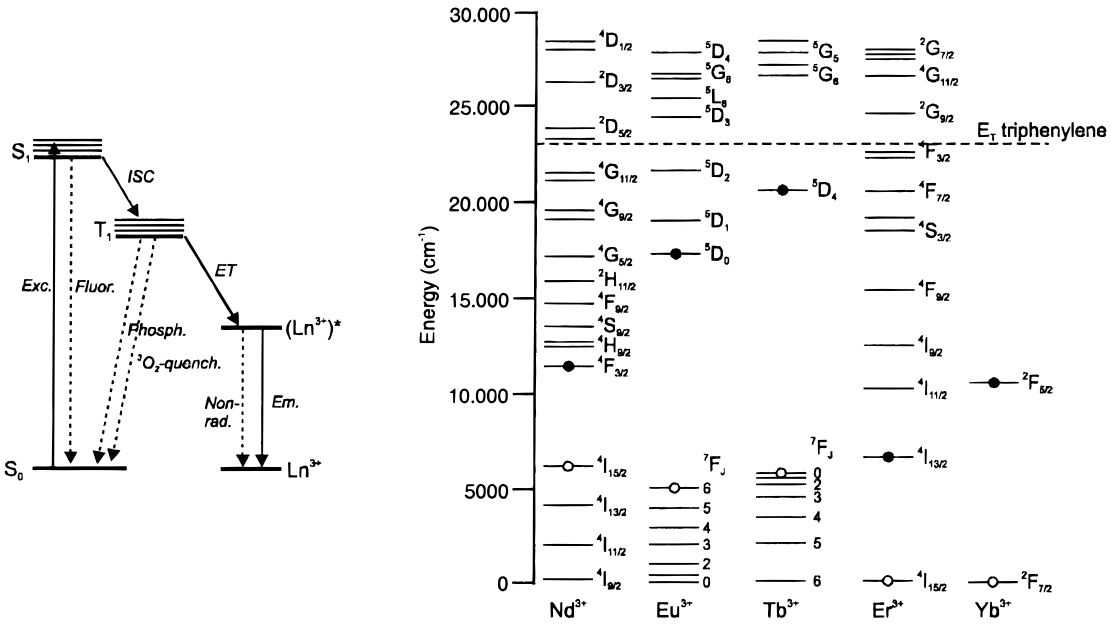

Figure 1. Left: Photophysical model describing the main pathways in the sensitization process. Right: Energy diagram of the 4f levels responsible for the lanthanide luminescence, where a filled circle denotes the lowest luminescent state and an open circle denotes the highest nonluminescent state (adapted from Stein, G.; Würzberg, E. *J. Chem. Phys.* **1975**, *62*, 208).

$$\phi_{se} = \phi_{isc}\phi_{et}\phi_{lum} \quad (1)$$

For an efficient population of the antenna triplet state upon excitation into its first singlet excited state, high absorption coefficients of the antenna at wavelengths in a suitable excitation window and a high intersystem crossing yield are required. The complexed lanthanide ion participates in the population of the triplet state by enhancing the intersystem crossing in the antenna chromophore via an external heavy atom effect.[9] The subsequent transfer of the excitation energy from the triplet state takes place via an electron exchange (Dexter) mechanism.[10] According to this theory, the energy-transfer rate is determined by the distance between the antenna and the lanthanide ion, and by the spectral overlap of the phosphorescence spectrum of the antenna and the absorption spectrum of the lanthanide ion. Dexter derived the following relationship between the distance and the energy-transfer rate:

$$k_{et} \sim e^{-2r/L} \quad (2)$$

where r is the distance between the donor and acceptor, in this case the antenna chromophore and lanthanide ion, and L is the sum of the van der Waals radii of the donor and acceptor. The energy-transfer process is strongly distance dependent and the transfer rate diminishes rapidly at distances larger than 5 Å. The triplet state of the antenna should be matched to the luminescent state of the receiving lanthanide ion to fulfill the energetic requirements, but approximately 2000 cm^{-1} higher in energy to ensure a fast and irreversible energy transfer.[5]

A general strategy in the design of luminescent lanthanide complexes is to synthesize a ligand that comprises lanthanide-complexing moieties, preferably charged oxygen donor atoms such as carboxylates,[4] and a sensitizer in close proximity to the bound lanthanide ion. Other examples of reported ligand systems for lanthanide complexation are cryptand-type ligands containing 2,2′-bipyridine,[11] DOTA aza-crown ether derivatives,[12] *m*-terphenyl-based ionophores,[13] and calix[4]arene-based ionophores.[14] Sensitizer-functionalized Eu^{3+} and Tb^{3+} complexes have already been applied as long-living luminescent probes in time-resolved fluoroimmunoassays,[15] whereas sensitizer-functionalized complexes of the near-infrared-emitting lanthanide ions Er^{3+}, Yb^{3+}, and Nd^{3+} are very promising not only for application in fluoroimmunoassays,[16] but also for use in laser systems,[17,18] and for amplification of light.[2,3]

Our ongoing research is concerned with the development of a polymer-based optical amplifier in which organic lanthanide complexes are incorporated in polymer waveguides. In the telecommunication network optical signal amplifiers are based on lanthanide-doped inorganic materials in which an optical transition of Er^{3+} is used for amplification of light around 1550 nm,[19] and an optical transition of Pr^{3+} is used for the amplification of light around 1300 nm.[20] Recently, a polymeric waveguide doped with neodymium chloride has been shown to amplify light of 1060 nm.[21]

Steemers et al. have shown that triphenylene can be incorporated into a calix[4]arene-based ionophore, and that the corresponding Eu^{3+} and Tb^{3+} complexes exhibit triphenylene-sensitized lanthanide luminescence.[22] The triphenylene antenna allows excitation up to 350 nm, and it has a high intersystem crossing quantum yield (0.89).[23] Oude Wolbers et al. have reported the synthesis and photophysical properties of *m*-terphenyl-based lanthanide complexes.[13] Recently, we have developed a synthesis route that allows the incorporation of a sensitizer into an *m*-terphenyl-based ionophore.[24,25] In this paper, we report the synthesis of an *m*-terphenyl-based ligand that has been functionalized with a triphenylene antenna chromophore (Chart 1), and a systematic study of the photophysical processes of the corresponding visible-light-emitting Eu^{3+} and Tb^{3+} complexes and near-IR-light emitting Nd^{3+}, Yb^{3+}, and Er^{3+} complexes. The present ligand is based on the *m*-terphenyl and offers eight oxygen donor atoms for complexation and shielding of the lanthanide ion: three bidentate oxyacetate moieties and two amide oxygens. The resulting complexes are overall neutral. The triphenylene antenna chromophore has been functionalized with an amide carbonyl to position it in close proximity of the lanthanide ion upon coordination of this functionality.

Results and Discussion

Synthesis. The triphenylene-functionalized ligand (H_3)**1** was synthesized in four steps starting from bis(amine) **5**[24] and

CHART 1

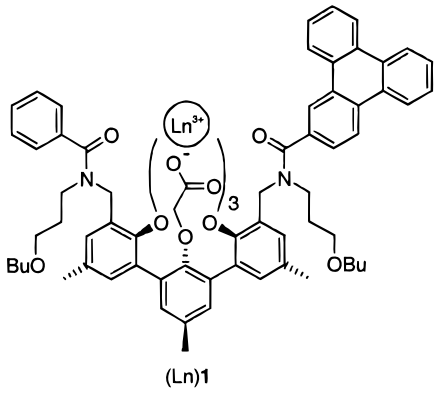

(Ln)**1**

Ln = Eu, Tb, Gd, Er, Yb, or Nd

triphenylene aldehyde **2**[22] (see Scheme 1). Reaction of bis(amine) **5** with 1.3 equiv of benzoyl chloride gave the mono(amide) **6** in 20−30% isolated yield. Triphenylene carboxylic acid **3** was synthesized in 80% yield by mild oxidation of triphenylene aldehyde **2**. Triphenylene carboxylic acid chloride **4** was prepared in situ with thionyl chloride ($SOCl_2$). After removal of the excess $SOCl_2$, the triphenylene carboxylic acid chloride **4** was reacted with mono(amide) **6** in dichloromethane in the presence of Et_3N, giving **7** in 60% yield. After quantitative hydrolysis of the *tert*-butyl esters of **7** with trifluoroacetic acid (TFA), the corresponding complexes were readily formed upon addition of the lanthanide nitrate salts to methanol solutions of the ligand in the presence of Et_3N as a base. FAB mass spectra indicate that the complexes have a 1:1 stoichiometry. The IR spectra confirm the presence of carboxylates.

Molecular Dynamics Studies. The structure of the (Ln)**1** complexes (Ln = Nd^{3+}, Eu^{3+}, Er^{3+}, Yb^{3+}) was minimized in the gas phase and subjected to molecular dynamics simulations (500 ps) in a cubic OPLS[26] box of methanol or DMSO using the CHARMM force field.[27] The simulations show that the structures of the complexes are comparable in both solvent boxes: all eight donor atoms from the ligand (three phenol ether oxygens (PhO), three carboxylate oxygens (OCO), and two amide oxygens (NCO)) are coordinated to the lanthanide ion, and one methanol or DMSO molecule is coordinated to the lanthanide ion. The PhO−Ln (typically 2.5 Å), OCO−Ln (typically 2.4 Å), and NCO−Ln (typically 2.3 Å) distances are comparable in this series of (Ln)**1** complexes, despite the differences in ionic radii of the various lanthanides. In the present complexes the coordination geometry is controlled not only by steric hindrance and Coulombic interactions, but also by the conformational restraints of the ligand system. In the (Ln)**1** complexes, the average distance from the center of the lanthanide ion to the *center* of the sensitizer is approximately 8 Å. The coordination of the amide carbonyl to the lanthanide ion positions the bottom phenyl ring of the triphenylene sensitizer at approximately 5 Å from the lanthanide ion.

Sensitized Lanthanide Emission. *a. (Eu)**1** and (Tb)**1**.* Upon excitation at 310 nm, the emission spectra of the (Eu)**1** complex in methanol show the typical narrow bands corresponding to the Eu^{3+}-centered $^5D_0 \rightarrow {}^7F_j$ transitions (solid line in Figure 2), with the strongest emission located around 615 nm originating from the $^5D_0 \rightarrow {}^7F_2$ transition. Scanning the excitation wavelength while monitoring the intensity of the Eu^{3+} emission at 615 nm shows which transitions from the ground state, directly or indirectly, lead to population of the Eu^{3+} $^5D_0$ luminescent state. The resulting excitation spectrum (dashed line in Figure 2) shows a maximum around 300 nm, closely resembles the absorption spectrum of the antenna, and proves that the lanthanide ion is excited via the triphenylene moiety.

The relative intensities and splitting of the (Eu)**1** emission bands are influenced by the symmetry of the ligand, and in particular by the symmetry of the first coordination sphere. Experimental data on a variety of Eu^{3+} complexes established that the emission band centered around 590 nm corresponding to the $^5D_0 \rightarrow {}^7F_1$ transition, which is a magnetic dipole transition, is relatively strong and largely independent of the coordination sphere, i.e., the ligand field. The emission band centered around 615 nm, corresponding to the $^5D_0 \rightarrow {}^7F_2$ transition, which is an electric dipole transition, is extremely sensitive to the symmetry of the coordination sphere and is therefore called *hypersensitive*. It has been established that the intensity ratio of the $^5D_0 \rightarrow {}^7F_2$ transition and the $^5D_0 \rightarrow {}^7F_1$ transition is a measure for the symmetry of the coordination sphere.[28] In a centrosymmetric environment the magnetic dipole $^5D_0 \rightarrow {}^7F_1$ transition of Eu^{3+} is dominating, whereas distortion of the symmetry around the ion causes an intensity enhancement of the *hypersensitive* $^5D_0 \rightarrow {}^7F_2$ transition. Complexes with an asymmetric coordination sphere such as lanthanide−tris(*β*-diketonate) complexes have $^7F_2/^7F_1$ intensity ratios ranging from 8 to 12, whereas an intensity ratio of 0.67 has been reported for the centrosymmetric Eu−tris(oxydiacetate) complex.[28] In the present case the $^7F_2/^7F_1$ intensity ratio for (Eu)**1** is 4. This value is significantly higher than 0.67, which is not surprising, since the structures obtained from molecular modeling simulations show that the first coordination spheres of the (Ln)**1** complexes have a (time-averaged) C_s symmetry.[29]

The (Eu)**1** spectrum at room temperature shows a splitting of the $^5D_0 \rightarrow {}^7F_1$ emission and the $^5D_0 \rightarrow {}^7F_2$ emission, and a single peak at 580 nm corresponding to the $^5D_0 \rightarrow {}^7F_0$ transition. Lowering the temperature to 77 K did not alter the shape and splitting of the emission bands (not shown). The values of the ligand field splittings are small, approximately 200 cm^{-1} for the $^7F_1$ state and 130 cm^{-1} for the $^7F_2$ state, which is due to the shielding of the 4f orbitals from the environment by an outer shell of 5s and 5p electrons.[4] The Eu^{3+} $^7F_0$ state is nondegenerate and cannot be split by the ligand field; therefore, the single peak at 580 nm indicates that there is only one (time-averaged) *luminescent* Eu^{3+} species in solution.

Photoexcitation of the antenna at 310 nm in the (Tb)**1** complex gives rise to the characteristic green Tb^{3+} emission corresponding to the $^5D_4 \rightarrow {}^7F_j$ transitions (solid line in Figure 3). The strongest emission is centered around 545 nm and corresponds to the hypersensitive $^5D_4 \rightarrow {}^7F_5$ transition. Monitoring the intensity of the 545 nm emission band, the excitation spectrum of (Tb)**1** proves the photosensitization via the antenna. The Tb^{3+} spectrum shows some fine structure within the emission bands, but they do not provide a basis for a reliable diagnostic probe of the symmetry of the complex, as is the case for the Eu^{3+} spectra.[30]

The time-resolved luminescence spectra show monoexponential decays with a luminescence lifetime of 0.86 ms for (Eu)**1** and 1.74 ms for (Tb)**1** in methanol (see Table 1). These lifetimes increase substantially in methanol-d_1, caused by the well-known sensitivity of the Eu^{3+} and Tb^{3+} luminescence toward solvent hydroxyl groups.[31] An empirical relationship has been established that estimates the number of coordinated methanol molecules (n):[32,33]

$$n = q(1/\tau_h - 1/\tau_d - k_{corr}) \qquad (3)$$

where q is 2.1 for Eu^{3+} and 8.4 for Tb^{3+}, τ_h is the luminescence lifetime of the complex in methanol-h_1, τ_d is the luminescence

SCHEME 1[a]

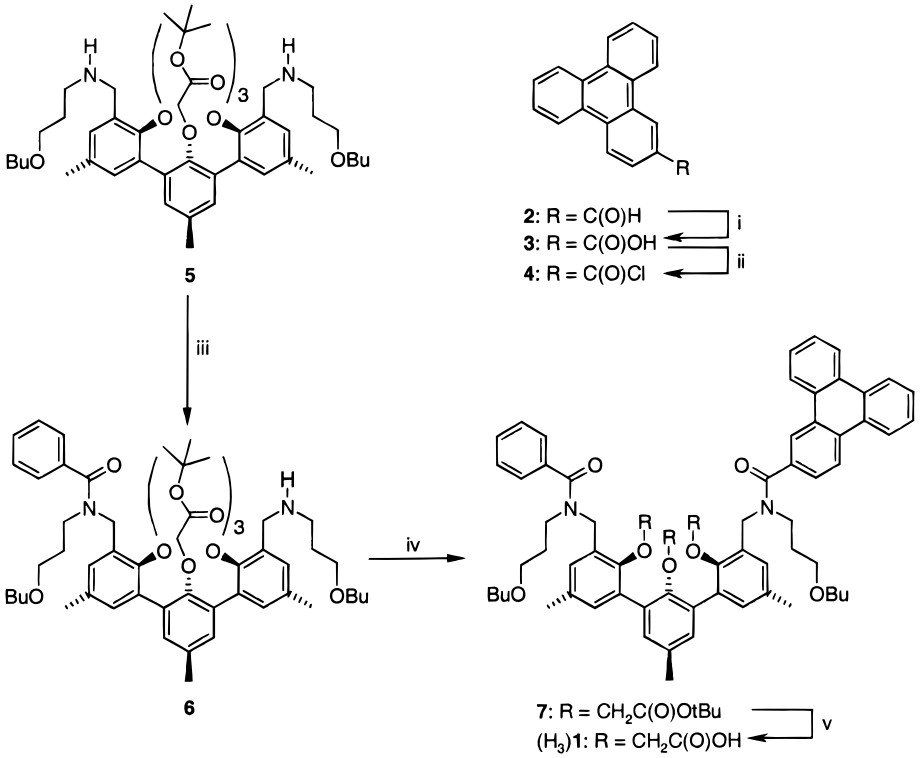

[a] Reagents and conditions: (i) H_2NSO_3H, $NaClO_2$, $CHCl_3$/acetone/water, 3 h, room temperature (80%); (ii) $SOCl_2$, reflux 4 h (100%); (iii) benzoyl chloride, Et_3N, CH_2Cl_2, 12 h, rt (20%); (iv) triphenylene acid chloride, Et_3N, CH_2Cl_2, 12 h, rt (70%); (v) TFA, 12 h, rt (100%).

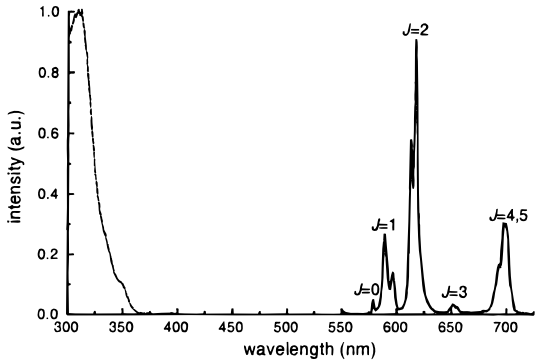

Figure 2. Excitation spectrum (dashed line, $\lambda_{em} = 615$ nm) and emission spectrum ($\lambda_{ex} = 310$ nm) of a 10^{-4} M solution of (Eu)**1** in methanol. The emission bands correspond to $^5D_0 \rightarrow {}^7F_j$ transitions and were recorded with a 1 nm emission bandwidth.

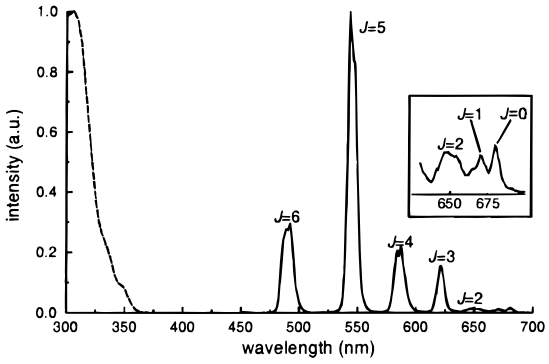

Figure 3. Excitation spectrum (dashed line, $\lambda_{em} = 545$ nm) and emission spectrum ($\lambda_{ex.} = 310$ nm) of a 10^{-4} M solution of (Tb)**1** in methanol. The emission bands correspond to $^5D_4 \rightarrow {}^7F_j$ transitions and were recorded with a 1 nm emission bandwidth. The inset shows a magnification of the emission bands between 625 and 700 nm.

lifetime of the complex in methanol-d_1, and k_{corr} is a term to correct for closely diffusing second-sphere methanol molecules, which is 0.125 ms^{-1} for Eu^{3+} and 0.03 ms^{-1} for Tb^{3+}.[33] The calculations show that approximately one methanol molecule is coordinated to the lanthanide ion (see Table 1). The coordination number of Eu^{3+} and Tb^{3+} complexes in solution is usually 9,[34] which implies that all eight donor atoms of the ligand are coordinated to the lanthanide ion. This is in excellent agreement with the results obtained from the molecular dynamics studies.

The efficiency of the overall sensitization process was established by determining the quantum yield of the sensitized emission, which is 0.03 for (Eu)**1** and 0.15 for (Tb)**1** in methanol. The emission spectra of these complexes in DMSO-h_6, a strongly coordinating aprotic solvent, closely resemble the spectra in methanol, but surprisingly the overall quantum yields are much lower: 0.02 for (Eu)**1** and 0.03 for (Tb)**1**. Time-resolved measurements showed that the luminescence lifetimes are longer in DMSO than in methanol-h_1 (see Table 1); therefore, the sensitization process of the (Eu)**1** and (Tb)**1** complexes in DMSO must be much less efficient than in methanol. The sensitization process will be discussed in more detail below.

TABLE 1: Luminescence Lifetimes of (Eu)1 and (Tb)1 Measured in Methanol-h_1 (τ_h), Methanol-d_1 (τ_d), and DMSO-h_6 (τ_h), Number of Coordinated Methanol-h_1 Molecules (n) Determined from Eq 1, and Overall Quantum Yield of Sensitized Emission (ϕ_{Se})[a]

complex	τ_h (ms)	τ_d (ms)	n	ϕ_{se}
(Eu)**1**	0.86[b]	2.21[c]	1.2 ± 0.5	0.03[b]
(Tb)**1**	1.74[b]	2.78[c]	1.6 ± 1.5	0.15[b]
(Eu)**1**	1.89[d]	nd	na	0.02[d]
(Tb)**1**	2.21[d]	nd	na	0.03[d]

[a] Excitation at 310 nm, 10^{-4} M solutions. [b] In methanol-h_1. [c] In methanol-d_1. [d] In DMSO-h_6.

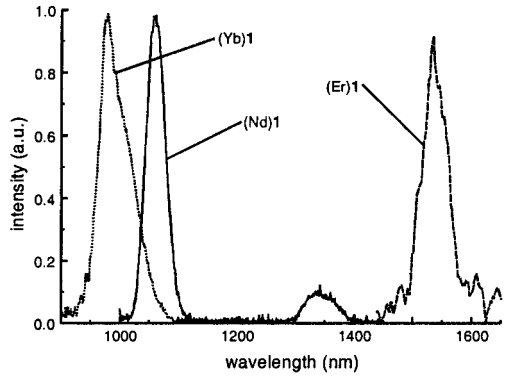

Figure 4. Emission spectra of 10^{-3} M solutions of the near-infrared-emitting complexes (Yb)**1**, (Nd)**1**, and (Er)**1** in DMSO-d_6 upon excitation at 320 nm recorded with a 15 nm emission bandwidth.

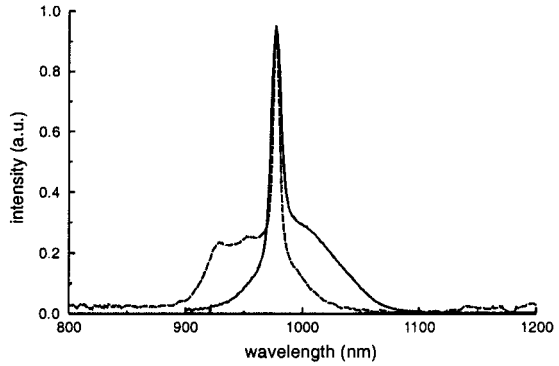

Figure 5. Absorption spectrum of a 10^{-2} M solution of (Yb)**1** in DMSO (dashed line) and emission spectrum (solid line) of a 10^{-3} M solution of (Yb)**1** in DMSO-d_6 upon laser excitation at 350 nm (Ar laser) recorded with a 6 nm emission bandwidth.

*b. (Nd)**1**, (Er)**1**, and (Yb)**1**.* The near-IR-emitting lanthanide complexes in DMSO-d_6 exhibit the typical line-like lanthanide emission upon excitation of the triphenylene antenna chromophore, as is depicted in Figure 4. Emission bands at 880 (not shown), 1060, and 1330 nm ($^4F_{3/2} \rightarrow {}^4I_{9/2}$, $^4I_{11/2}$, and $^4I_{13/2}$ transitions, respectively) are observed for (Nd)**1**. The strongest emission is observed at 1060 nm, whereas the emissions at 880 and 1330 nm are weaker. The shape of the emission bands and the relative intensities are in agreement with previously reported spectra of organic Nd^{3+} complexes in solution.[13,16,35] A single emission band centered at 1540 nm ($^4I_{13/2} \rightarrow {}^4I_{15/2}$ transition) is observed for (Er)**1**. No emission was observed from higher excited states, such as green emission at 545 nm corresponding to the $^4S_{3/2} \rightarrow {}^4I_{15/2}$ transition, despite the fact that these states are populated via the antenna triplet state. Apparently, the higher excited states relax nonradiatively to the $^4I_{13/2}$ state, from which radiative decay is observed. Upon excitation of (Yb)**1** at 310 nm, sensitized emission was observed at 980 nm ($^2F_{5/2} \rightarrow {}^2F_{7/2}$ transition). A shoulder seems to be present at the lower energy side of the 980 nm emission band, which is indicative of splitting of the $^2F_{7/2}$ manifold by the ligand field. Using laser excitation, an emission spectrum of (Yb)**1** was obtained (solid line in Figure 5) with a higher resolution (6 nm) in which a sharp peak at 977 nm (10 235 cm^{-1}) is observed with a broad shoulder at 1005 nm (9950 cm^{-1}). The same sharp peak at 977 nm is observed in the absorption spectrum (dotted line in Figure 5) together with a broad shoulder at 940 nm (10 600 cm^{-1}), which means that also the $^2F_{5/2}$ manifold is split by the ligand field. The shapes of the luminescence and absorption spectra are similar to those of the reported spectra of Yb^{3+} in both organic and inorganic matrixes.[36,37,38]

TABLE 2: Luminescence Lifetimes of the Near-IR-Emitting (Ln)1 Complexes in DMSO-h_6 ($\tau_h = 1/k_h$) and DMSO-d_6 ($\tau_d = 1/k_d$), as Well as the Natural Lifetimes ($\tau_0 = 1/k_0$)[a]

complex	τ_h (μs)	k_h (s^{-1})	τ_d (μs)	k_d (s^{-1})	τ_0 (ms)	k_0 (s^{-1})
(Yb)**1**	9.4	1.1×10^5	18.6	0.54×10^5	2.0	500
(Er)**1**	2.4	4.2×10^5	3.4	2.9×10^5	14.0	71
(Nd)**1**	1.4	7.1×10^5	2.5	4.0×10^5	0.25	4000

[a] Excitation at 337 nm, 10^{-3} M solutions.

TABLE 3: Quantum Yields of the Triphenylene Antenna Fluorescence in Methanol[a]

complex	$\phi_{antenna}$	complex	$\phi_{antenna}$
7	0.019	(Yb)**1**	0.012
(Eu)**1**	0.0054	(Er)**1**	0.0095
(Tb)**1**	0.0086	(Nd)**1**	0.0095
(Gd)**1**	0.015		

[a] Excitation at 310 nm, 10^{-4} M solutions.

The luminescence decay curves obtained from time-resolved luminescence experiments could be fitted monoexponentially with time constants in the range of microseconds (see Table 2). The luminescence lifetime of (Yb)**1** in DMSO-h_6 is the longest (9.6 μs), followed by that of (Er)**1** (2.4 μs), and that of (Nd)**1** (1.5 μs). The sensitivity of the near-IR luminescent complexes toward quenching by the C−H vibrations becomes apparent when the solvent is changed to DMSO-d_6. In DMSO-d_6 the luminescence lifetimes are significantly longer due to the fact that the C−D vibrations of the coordinated DMSO-d_6 molecule are less efficient quenchers of the lanthanide excited state than the C−H vibrations of a DMSO-h_6 molecule. According to the energy gap law[39] the smaller the number of vibrational quanta that are required to match the energy gap between the lowest luminescent state and the highest nonluminescent state of the lanthanide ion, the more effective the vibronic quenching will be. For the C−H vibration with vibrational quanta of 2950 cm^{-1}, the number of harmonics (n_h) necessary to match the energy gap is largest for Yb^{3+} (n_h = 3−4), followed by Er^{3+} (n_h = 2−3), and smallest for Nd^{3+} (n_h = 1−2). As a consequence, the quenching rate constant by the solvent C−H vibrations is higher for (Nd)**1** than for (Yb)**1**. For comparison, the energy gap of Eu^{3+} (with n_h = 6−7) and Tb^{3+} (with n_h = 8−9) is much larger than the energy gap of the near-IR-emitting lanthanide ions, which renders them far less sensitive toward C−H quenching. The radiative rate constants (k_0), i.e., the rate of spontaneous emission, of Er^{3+} and Yb^{3+} in these type of complexes in DMSO have been added to Table 2. A typical radiative rate constant of Nd^{3+} has also been added to Table 2.[40] Since the observed rate constant k is the sum of the natural radiative rate constant k_0 and the nonradiative rate constant k_{nonr}, it is obvious from Table 2 that for the near-IR-emitting ions k is dominated by nonradiative deactivation of the luminescent state. This competition between nonradiative and radiative decay is most dramatic for Er^{3+}, because this ion has a very low k_0 of 71 s^{-1}.

Antenna Fluorescence and Phosphorescence. The first step of the sensitization pathway is the population of the triphenylene triplet state ($^3\pi\pi^*$) via its singlet excited state ($^1\pi\pi^*$). In this step fluorescence and radiationless deactivation from the triphenylene $^1\pi\pi^*$ state compete with the spin-forbidden conversion to the $^3\pi\pi^*$ state. The shapes of the UV absorption spectra of the (Ln)**1** complexes in methanol are similar to that of ligand **7**, indicating that the lanthanide ion does not significantly influence the energy of the triphenylene $^1\pi\pi^*$ state. The $^1\pi\pi^*$ state energy of 29 000 cm^{-1} (345 nm) was determined from the 0−0 transition, which is clearly discernible in the absorption

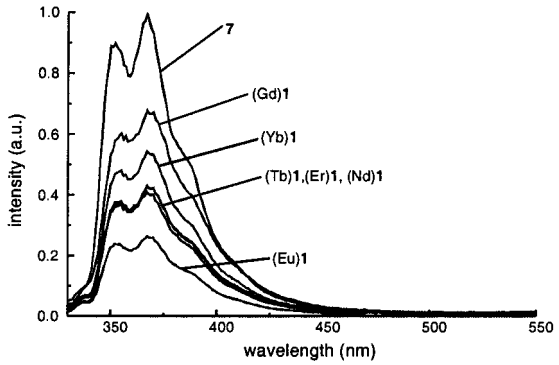

Figure 6. Fluorescence spectra of the triphenylene antenna in ligand **7** and in the (Ln)**1** complexes in methanol upon excitation at 310 nm. The intensities are relative to the fluorescence intensity of **7**.

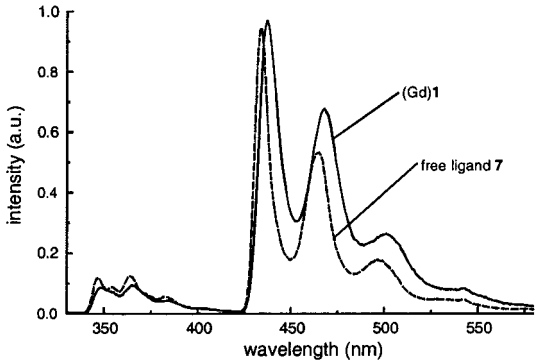

Figure 7. Fluorescence and phosphorescence spectra of the triphenylene antenna of **7** and (Gd)**1** taken in a methanol−ethanol glass at 77 K ($\lambda_{exc} = 310$ nm).

spectrum. Upon excitation of the (Ln)**1** complexes in methanol at 310 nm, a structured fluorescence band is observed at 375 nm that corresponds to fluorescence of the triphenylene moiety. Figure 6 shows the fluorescence intensities of the (Ln)**1** complexes relative to the free ligand **7**. The fluorescence quantum yields are summarized in Table 3. The presence of the lanthanide ion in close proximity of the antenna reduces the fluorescence intensity, but the effect is not the same for all the lanthanide ions. The fluorescence quantum yield of ligand **7** is 0.019, whereas the fluorescence quantum yields of the (Ln)**1** complexes are even lower, <0.01. The fluorescence quantum yields are low, which is not surprising, since triphenylene has an intrinsically high intersystem crossing quantum yield.[23]

The luminescence spectrum of (Gd)**1** in a methanol/ethanol glass at 77 K shows strong phosphorescence bands next to very weak fluorescence bands. Since Gd^{3+} has no energy levels below 32 000 cm^{-1}, Gd^{3+} cannot accept any energy from the triphenylene triplet state. The $^3\pi\pi^*$ state energy of 22 830 cm^{-1} of the triphenylene moiety was determined from the 0−0 transition in the phosphorescence spectrum (see Figure 7). This value is approximately 600 cm^{-1} lower in energy than the $^3\pi\pi^*$ state of unfunctionalized triphenylene (23 400 cm^{-1}) and is caused by the electron-withdrawing amide carbonyl at the 2-position.

Compared to the phosphorescence spectrum of the free ligand **7**, the antenna phosphorescence bands of (Gd)**1** have slightly shifted to the red. Furthermore, the decrease of the antenna fluorescence intensity of (Gd)**1** is accompanied by an increased phosphorescence intensity. An *external heavy atom effect* can be induced by a heavy (paramagnetic) metal ion in close proximity of a chromophore, and increases the intersystem crossing yield of the chromophore, which results in a reduction of the fluorescence intensity and a concomitant increase in the phosphorescence intensity. This effect has been attributed to an enhanced spin−orbit coupling of the system which relaxes the selection rules for electronic transitions, but also to an exchange interaction of metal-unpaired electrons with the π-electrons of the organic chromophore. Tobita and co-workers[9] have studied the influence of different lanthanide ions on the photophysical properties of the ligand (the antenna) in lanthanide−tris(methylsalicylate) and lanthanide−tris(benzoyltrifluoroacetonato) complexes. They found that the decrease of the antenna fluorescence intensity depended on the magnetic properties of the lanthanide ion. The paramagnetic Gd^{3+} ion was found to lower the antenna triplet-state lifetime more than the diamagnetic Lu^{3+} and La^{3+} ions. If these results were solely caused by spin−orbit coupling, then the effect should have increased with increasing atomic number *Z*. Since this was not the case, an additional exchange mechanism between the metal-unpaired electrons and the chromophore electrons was proposed. The exchange leads to mixing of the chromophore singlet state and triplet state, ultimately resulting in more allowed singlet−triplet and triplet−singlet conversions. Also in the present case the effect, i.e., the reduction of the antenna fluorescence, does not increase with increasing *Z*, which implies that a paramagnetic exchange mechanism may also be predominant.

In the case of (Eu)**1**, which has the lowest antenna fluorescence intensity, a photon-induced electron transfer may also play a role in the deactivation of the singlet excited state. Instead of radiative decay to the ground state, or intersystem crossing to the triplet state, an electron is transferred to the Eu^{3+} ion upon excitation of the antenna into its singlet excited state, resulting in the transient formation of an antenna radical cation and Eu^{2+}. One of the reasons for the possible occurrence of this competing process[41] is the low reduction potential of Eu^{3+} in comparison with other trivalent lanthanide ions.[42]

Intramolecular Energy Transfer Process. *a. (Eu)1 and (Tb)1.* Since the energy transfer takes place through the triphenylene triplet state, oxygen may compete with the lanthanide ion as the acceptor for the excitation energy, and as a result the triplet state is quenched. In that case less lanthanide luminescence will be observed. The effect of oxygen on the sensitized luminescence intensity gives an indication of the energy-transfer rate, since the competing oxygen quenching rate is equal to the product of the diffusion-controlled quenching rate constant and the oxygen concentration ($k_{diff}[O_2]$). However, deoxygenation of the (Eu)**1** and (Tb)**1** methanol solutions did not influence the luminescence intensity, which means that k_{et} exceeds 10^7 s^{-1}.[43]

The energy-transfer process was further studied by probing the antenna's triplet state directly with the aid of transient absorption spectroscopy. To obtain the triplet−triplet absorption spectra of the complex, samples of (Gd)**1** in deoxygenated DMSO were excited with 335 nm pulses and the changes in absorbance resulting from the population of the long-lived triplet state were monitored. As mentioned before, the (Gd)**1** complex enables the study of the photophysical behavior of the antenna in the presence of a lanthanide ion, but in the absence of energy transfer. The transient absorption spectrum of (Gd)**1** (see Figure 8) shows features at 360 and 440 nm, which are very similar to the transient absorption spectrum of unfunctionalized triphenylene, but slightly broadened. These absorption bands are due to triplet−triplet absorptions and can therefore be used to monitor the lifetime of the triplet state, which was 15.2 μs in the (Gd)**1** complex. This lifetime is the lifetime of the antenna's

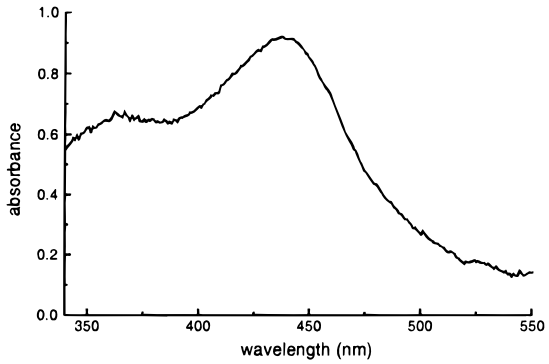

Figure 8. Transient absorption spectrum of (Gd)**1** in deoxygenated methanol recorded 100 ns after the laser pulse (340 nm, energy <1 mJ).

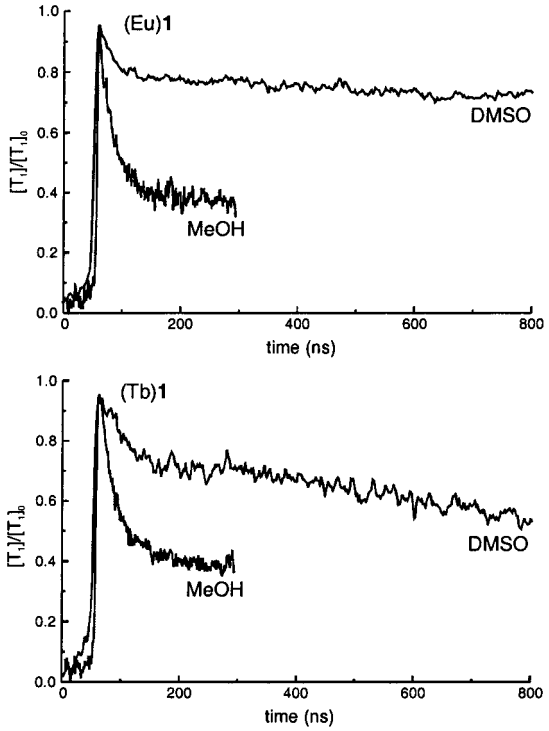

Figure 9. Kinetics of the transient absorption measurements obtained by singular value decomposition of the resulting datasets. The pump wavelength was 340 nm (<1 mJ/pulse). The corresponding transient absorption spectra were similar to the one shown in Figure 8. Top: (Eu)**1** in deoxygenated DMSO and methanol. Bottom: (Tb)**1** in deoxygenated DMSO and methanol.

triplet state in the absence of energy transfer, yielding a k_T of 6.6×10^4 s^{-1}.

The transient absorption spectra of the Tb(**1**) and Eu(**1**) complexes in the submicrosecond domain show interesting details about the energy-transfer process in DMSO and methanol. In DMSO the same absorption spectra are observed as for the (Gd)**1** complex, but the triplet-state kinetics of the antenna have become biexponential (see Figure 9): besides a "slow" component (76%) having the same rate constant as observed in Gd(**1**), a second small component (24%) is observed, which has a much faster decay (26 ns for Tb(**1**) and Eu(**1**)). The long triplet lifetimes would suggest that energy transfer to the lanthanide ion is extremely slow and an oxygen sensitivity of the lanthanide luminescence should have been observed. However, the intensity of the luminescence of both (Eu)**1** and (Tb)**1** is not influenced by deoxygenation. We therefore attribute this behavior to the presence of two distinct (conformational)

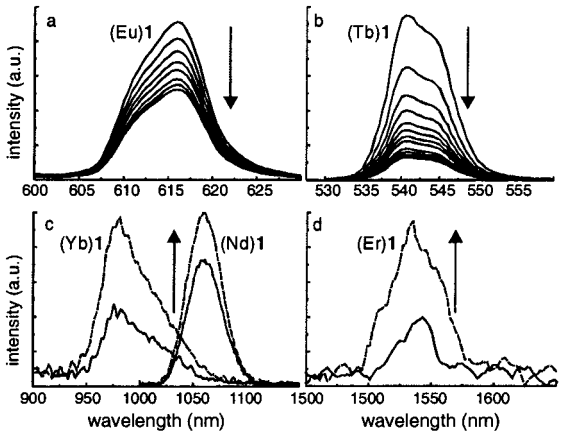

Figure 10. (a) Quenching of the 615 nm emission band of Eu^{3+} by piperylene. (b) Quenching of the 545 nm emission band of Tb^{3+} by piperylene. The arrows denote the effect of the increasing piperylene concentration in methanol. (c) Enhancement of the 980 nm emission band of Yb^{3+} and 1060 nm emission band of Nd^{3+} upon deaeration. (d) Enhancement of the 1550 nm emission band of Er^{3+} upon deaeration. The arrows denote the effect of deaeration of the DMSO-d_6 solutions.

populations of complexes: one in which energy transfer is absent and which is responsible for the observed long-lived triplets, and one in which the energy transfer to the lanthanide ion is relatively fast (responsible for the fast component), resulting in the sensitized luminescence. This is in line with the surprisingly low quantum yields of sensitized luminescence of the complexes in DMSO. According to our transient absorption measurements the majority of complexes do not display efficient energy transfer. Changing to methanol as the solvent, the antenna triplet-state kinetics show the same biexponential behavior as in DMSO, but the contribution of the fast component has increased to 65%. The corresponding short-lived triplet lifetime components are 29 and 26 ns for Tb(**1**) and Eu(**1**), respectively. Obviously, the equilibrium between the dark and the luminescent forms of the complexes has been shifted toward the luminescent side. Indeed, we already noted that in methanol the overall luminescence quantum yields are higher than in DMSO.

To substantiate the proof for the presence of two distinct forms of complexes in solution, experiments with an external triplet quencher were performed. *cis*-Piperylene has a triplet state of 20 070 cm^{-1},[23,44] which is approximately 2800 cm^{-1} lower than that of triphenylene. Addition of increasing concentrations of piperylene to methanol solutions of (Eu)**1** and (Tb)**1** quenched the sensitized lanthanide luminescence upon excitation of the antenna at 310 nm (see Figure 10a,b). This effect is more pronounced for Tb^{3+} than for Eu^{3+}, which may indicate that the energy-transfer rate to Eu^{3+} is faster. With the Stern−Volmer equation 4 the lifetime of the quenched species, i.e., the triphenylene triplet state, can be calculated. In eq 4, I_0 is the

$$I_0/I = 1 + k_{diff}\tau_T[Q] = 1 + K_{sv}[Q] \qquad (4)$$

lanthanide luminescence intensity without quencher, I is the lanthanide luminescence intensity, k_{diff} is the diffusion-controlled quenching rate constant, τ_T is the lifetime of the triphenylene triplet state, [Q] is the concentration of the quencher, and K_{sv} is the product of k_{diff} and τ_T, the so-called Stern−Volmer constant. If the luminescence intensities are plotted against the quencher concentration, the slope of the fitted data is equal to the Stern−Volmer constant K_{sv} (see Figure 11). When for k_{diff} a value of 10^{10} M^{-1} s^{-1} is taken,[23] the lifetime of the antenna

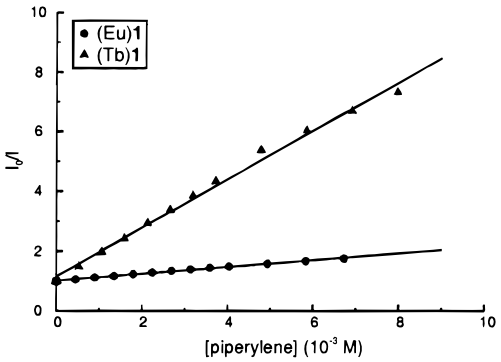

Figure 11. Stern−Volmer plot of quenching of triphenylene-sensitized Eu^{3+} and Tb^{3+} emission by piperylene: $I_0/I = 1 + k_{diff}\tau_{triplet}[Q] = 1 + K_{sv}[Q]$.

TABLE 4: Quenching of Sensitized (Ln)1 Luminescence by Piperylene (pip) or Oxygen (Ox)[a]

complex	τ_T (ns)	k_{ET} (s^{-1})	relative k_{ET} (s^{-1})
(Eu)**1** (pip)	11.3	8.0×10^7	100
(Tb)**1** (pip)	81.1	1.0×10^7	13
(Nd)**1** (ox)	76.1	1.3×10^7	16
(Er)**1** (ox)	263.0	3.8×10^6	5
(Yb)**1** (ox)	202.2	4.9×10^6	6

[a] Tabulated are the triphenylene triplet-state lifetimes (τ_T) using the Stern−Volmer equation and the energy-transfer rates (k_{et}).

triplet state can be calculated. This resulted in an antenna triplet lifetime of 11.3 ns for (Eu)**1** and 81.1 ns for (Tb)**1**. Since the antenna triplet lifetime is 15.2 μs in the absence of energy transfer (τ_T of (Gd)**1**), the deactivation of the antenna triplet is dominated by the rate of energy transfer to the lanthanide ion (k_{et}), and thus it follows that

$$k_{et} = 1/\tau_T \tag{5}$$

The intramolecular energy-transfer rate in (Eu)**1** is 8.0×10^7 s^{-1}, and 1.0×10^7 s^{-1} in (Tb)**1** (see Table 4).

Another way of studying the energy transfer is to monitor the early stages of the lanthanide luminescence using a streak camera and pulsed laser excitation. During the time that the energy transfer from the antenna to the lanthanide ion is in progress, the lanthanide luminescence intensity is expected to rise with a rate equal to the rate of the energy transfer. In these measurements it was found that the first 200 ns of the detected luminescence was completely dominated by the antenna fluorescence. Although the fluorescence has a low quantum yield, it has a very high radiative rate (i.e., the photons emitted per unit time) compared to the lanthanide luminescence. Therefore, on this short time scale, the lanthanide luminescence is relatively weak compared to the antenna fluorescence. After the antenna fluorescence signal had disappeared, no rise in the Tb^{3+} emission at 545 nm was observed for (Tb)**1**, signifying that the energy transfer to this ion is complete within 200 ns. This means that k_{et} exceeds 2×10^7 s^{-1} (on the basis of 99% energy transfer after 200 ns).

The (Eu)**1** complex exhibited an interesting behavior. After the disappearance of the antenna fluorescence, it shows emission from its $^5D_1$ state at 530 nm. This state decays with a time constant of 2.1 μs, being converted nonradiatively into the $^5D_0$ state that is responsible for the typical Eu^{3+} emission observed in steady-state measurements (main emission at 615 nm), and radiatively to the ^7F_j manifold. This behavior is known for the sensitized emission of Eu^{3+} if the donating triplet level is above the $^5D_1$ as in the present case.[6,7] The energy transfer from the antenna to the Eu^{3+} ion is faster than 2×10^7 s^{-1}.

The transient absorption measurements, the piperylene quenching experiment, and the luminescence rise time measurements, all show that the energy-transfer rates in the (Eu)**1** and (Tb)**1** complexes are on the order of 10^7-10^8 s^{-1}. The results of these measurements support the hypothesis that two distinct conformations of the complexes occur in solution: one in which the energy transfer to the lanthanide ion does not occur and which is responsible for the long-lived triplet lifetime observed by transient absorption spectroscopy, and one in which energy transfer is fast and which is responsible for the short-lived triplet lifetime. In the nonluminescent isomer the antenna and lanthanide ion are probably remote or the orientation of the lanthanide ion with respect to the antenna π-plane is unfavorable for energy transfer to occur.[45] In methanol there seems to be an equal distribution between the luminescent and nonluminescent conformational isomers of the complexes. This explains the relatively low luminescence quantum yields that were measured for (Eu)**1** and (Tb)**1** in methanol: 0.03 and 0.15, respectively. On the basis of measured luminescence lifetimes, the ISC yield of the antenna near unity, and an assumed complete energy transfer, the luminescence quantum yields can be expected to be as high as 0.29 for (Eu)**1** and 0.44 for (Tb)**1**.[46] As mentioned before, the overall luminescence quantum yields of these complexes in DMSO are even lower, 0.02 for (Eu)**1** and 0.03 for (Tb)**1**. In this solvent the nonluminescent conformational isomer seems to be dominating (according to the transient absorption measurements), resulting in an overall very inefficient energy-transfer process. The decrease in the luminescence quantum yield when the solvent is changed from methanol to DMSO is less dramatic for (Eu)**1** than for (Tb)**1**, because the significant increase of the (Eu)**1** luminescence lifetime partly compensates the inefficiency of the energy-transfer process. For the (Eu)**1** complex in methanol and DMSO, energy may also be lost in the step preceding the energy transfer, i.e., the population of the triplet state. On the basis of the observation that the antenna fluorescence intensity of (Eu)**1** (ϕ_{flu} = 0.0054) is lower than the antenna fluorescence intensity of (Tb)**1** (ϕ_{flu} = 0.0086), a photon-induced electron transfer (a metal-to-ligand charge transfer (MLCT)) may also compete with the intersystem crossing to the triplet state in the former complex. Since, in general, the deactivation of such an MLCT state does not result in the population of the Eu^{3+} $^5D_0$ excited state,[41] a photon-induced electron-transfer process will reduce the overall luminescence quantum yield.[47]

The Stern−Volmer plot of the triplet quenching experiments only provides information on the *luminescent* conformational isomer of the complexes. From these experiments it was concluded that the energy-transfer rate is significantly faster in the (Eu)**1** complex (8.0×10^7 s^{-1}) than in the (Tb)**1** complex (1.0×10^7 s^{-1}). However, on the basis of transient absorption measurements the energy-transfer rates were approximately the same for the (Eu)**1** and (Tb)**1** complexes (3.8×10^7 s^{-1}). The explanation for this is that the values obtained from the piperylene quenching experiment are lower limits, because it was found that piperylene also quenched the luminescent states of Eu^{3+} and Tb^{3+}, albeit to different extents.[48] Furthermore, the quenching of Tb^{3+} is more efficient, because the triplet state of *cis*-piperylene (20 070 cm^{-1}) is just below the $^5D_4$ state of Tb^{3+} (20 400 cm^{-1}), whereas it is higher in energy than the $^5D_1$ and $^5D_0$ states of Eu^{3+} (19 000 and 17 500 cm^{-1}, respectively). As a result, the calculated energy-transfer rate for (Tb)**1** as obtained from the quenching experiment has been underestimated more than the calculated energy-transfer rate of (Eu)**1**.

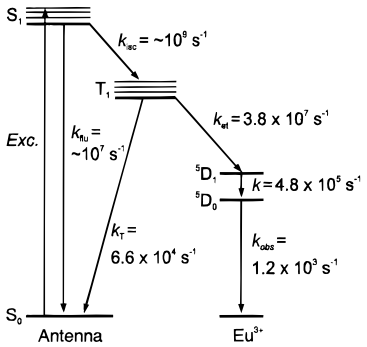

Figure 12. Schematic representation of the photophysical processes leading to sensitized luminescence of (Eu)**1** together with the rate constants of the processes.

The photophysical processes and the rate constants in (Eu)**1** are summarized in Figure 12.

*b. (Nd)**1**, (Er)**1**, and (Yb)**1**.* The energy-transfer rates were determined in the near-IR-emitting complexes by measuring the influence of oxygen on the sensitized luminescence. The luminescence intensity is enhanced by 35% for (Nd)**1**, 120% for (Er)**1**, and 90% for (Yb)**1** upon deoxygenation of the DMSO-d_6 solutions (see Figure 10c,d), indicating that, contrary to the (Eu)**1** and (Tb)**1** complexes, oxygen quenching is competing with the energy transfer to the lanthanide ion. The Stern−Volmer equation can be used to estimate the antenna triplet-state lifetimes and the energy-transfer rates from this oxygen dependence. The diffusion-controlled quenching constant k_{diff} was taken as 10^{-10} $M^{-1}s^{-1}$, and the oxygen concentration in DMSO was taken as 0.47 mM.[23] The results are summarized in Table 4. The energy transfer to Yb^{3+} and Er^{3+} is significantly slower than the energy transfer to Nd^{3+}.

Changing the solvent to methanol-d_4 would shift the equilibrium between the dark and luminescent conformational isomers of the complex toward the luminescent conformational isomer, as has been shown for (Eu)**1** and (Tb)**1**, and would thus increase the quantum yield of the energy transfer (ϕ_{et}). Unfortunately, the luminescence lifetimes of (Nd)**1**, (Yb)**1**, and (Er)**1** are significantly lower in methanol-d_4: for example, the lifetimes of (Nd)**1** and (Er)**1** in methanol-d_4 are 0.89 and 1.16 μs, respectively. Thus, changing the solvent from DMSO-d_6 to methanol-d_4 will not increase the *overall* luminescence quantum yield (ϕ_{se}).

A special case is Yb^{3+}, since it has only one excited state ($^2F_{5/2}$), which is approximately 10 000 cm^{-1} lower in energy than the antenna triplet state. It has been argued that the spectral overlap is therefore negligible.[49] On the basis of the fact that, like Eu^{3+}, Yb^{3+} is relatively easily reduced to Yb^{2+},[50] an internal redox mechanism has been proposed for the sensitized Yb^{3+} luminescence that takes place through the singlet state of the antenna chromophore.[49] The driving force $-\Delta G_{RET}$ of such a redox energy transfer can be estimated with the equation $\Delta G_{RET} = E(\text{Triph}^{\bullet+}/\text{Triph}) - E_{\text{Triph}^*} - E(Yb^{3+}/Yb^{2+})$. However, this mechanism is not operative in our system. In a cyclic voltammetry measurement on a reference Yb^{3+} complex[51] similar to (Yb)**1** in DMSO, no reduction was observed up to −1.90 V vs SCE. Since the oxidation potential of triphenylene is 1.55 V vs SCE,[52] $E(\text{Triph}^{\bullet+}/\text{Triph}) - E(Yb^{3+}/Yb^{2+})$ is >3.45 eV, whereas the energy of the triphenylene singlet excited state (E_{Triph^*}) is 3.6 eV. Therefore, there is almost no driving force for the photoinduced redox reaction in our system. Moreover, if the redox energy-transfer mechanism is operative, then the fluorescence of the triphenylene moiety of (Yb)**1** must be competing not only with intersystem crossing, but also with the energy transfer. Our photophysical data, i.e., the triphenylene fluorescence quantum yield and the oxygen dependence of the sensitized emission, show that the energy-transfer takes place via the triplet state. Therefore, the energy transfer mechanism is most likely an electron-exchange mechanism. The extremely small spectral overlap of the antenna phosphorescence spectrum and the Yb^{3+} absorption spectrum causes the energy transfer to be slower than, for example, in the (Eu)**1** and (Nd)**1** complexes. The recently reported sensitized near-infrared Nd^{3+}, Yb^{3+}, and Er^{3+} luminescence by energy transfer from the dye fluorescein was shown to be oxygen sensitive.[16] Especially, the sensitized Yb^{3+} luminescence was very sensitive to oxygen, indicating not only that the energy-transfer process proceeds via the triplet state, but also that it is very slow.

Conclusion

This study has shown that the (Ln)**1** complexes exist in solution in two conformational isomers: one in which energy transfer does not take place, and one in which the energy transfer takes place, resulting in sensitized luminescence. Using quenching experiments to study this luminescent species, it was found that the energy-transfer process is fast in the (Eu)**1** and (Tb)**1** complexes (no oxygen dependence), whereas it is slower in the near-IR-emitting complexes (oxygen dependence). The energy-transfer rates should be improved by direct coordination of the antenna chromophore to the lanthanide ion, which would reduce not only the distance between the donor and acceptor, but also the conformational freedom of the antenna relative to the lanthanide ion. An improvement of the spectral overlap of the near-IR-emitting lanthanide ions (especially Yb^{3+}) and the antenna should be achieved by incorporating antenna chromophores with lower lying triplet states. We have shown that dyes such as fluorescein can sensitize Er^{3+}, Yb^{3+}, and Nd^{3+} emission,[3,16] and we are currently investigating the incorporation of these dyes in *m*-terphenyl-based ligands.

Experimental Section

General Synthesis. Melting points were determined with a Reichert melting point apparatus and are uncorrected. Mass spectra were recorded with a Finnigan MAT 90 spectrometer using *m*-NBA (nitrobenzyl alcohol) as a matrix, unless stated otherwise. IR spectra were obtained using a Biorad 3200 or a Nicolet 5SXC FT-IR spectrophotometer. ^1H NMR and ^{13}C NMR spectra were recorded with a Bruker AC 250 spectrometer in $CDCl_3$ using residual solvent peaks as the internal standard, unless stated otherwise. Preparative column chromatography separations were performed on Merck silica gel (particle size 0.040−0.063 mm, 230−400 mesh). CH_2Cl_2, $CHCl_3$, and hexane (mixed isomers) were distilled from $CaCl_2$ and stored over molecular sieves (4 Å). Ethyl acetate was distilled from K_2CO_3 and stored over molecular sieves (4 Å). Triethylamine (Et_3N) was distilled in vacuo and stored over KOH. Acetone and methanol were of analytical grade and were dried over molecular sieves prior to use (4 and 3 Å, respectively). All reactions were carried out under an argon atmosphere. Standard workup means that the organic layers were finally washed with water, dried over magnesium sulfate ($MgSO_4$), filtered, and concentrated to dryness in vacuo.

Triphenylene-2-carboxylic Acid 3. To a solution of triphenylene-2-carboxaldehyde **2** (0.60 g, 2.34 mmol) in a mixture of $CHCl_3$ (30 mL) and acetone (90 mL) were subsequently added a solution of H_2NSO_3H (0.50 g, 5.16 mmol) in water (1 mL) and a solution of $NaClO_2$ (0.50 g, 6.50 mmol) in water (1 mL). The resulting mixture was stirred for 3 h at room

temperature, after which it was concentrated in vacuo until the product precipitated. The solid was filtered off, washed thoroughly with water, and dried in vacuo. The product was obtained as an off-white solid, yield 80%. Mp: >250 °C. ^{1}H NMR (DMSO-d_6): δ 9.29 (s, 1H), 8.94−8.74 (m, 5H), 8.19 (d, 1H, J = 8.0 Hz), 7.80−7.68 (m, 4H). ^{13}C NMR: 168.1, 133.2, 130.7, 130.2−128.2, 125.5−124.2. IR (KBr): 1684 cm^{-1} (ν_{COOH}). Mass spectrum (EI): m/z = 272.0 [M$^+$, calcd 272.1]. Anal. Calcd. for $C_{19}H_{12}O_2$: C, 83.81, H, 4.44. Found: C, 83.87; H, 4.46.

Mono(amide) Terphenyl (6). To a solution of bis(amine) **5** (2.0 g, 2.11 mmol) and Et_3N (0.58 mL, 4.2 mmol) in CH_2Cl_2 (200 mL) was slowly added a solution of benzoyl chloride (0.41 g, 2.95 mmol) in CH_2Cl_2 (50 mL). The resulting solution was stirred overnight at room temperature. Subsequently, CH_2Cl_2 was added (100 mL), and the reaction mixture was washed twice with 5% K_2CO_3, followed by standard workup. The crude product was purified by flash column chromatography (MeOH/CH_2Cl_2, 1:9) to give mono(amide) **6** as a colorless oil, yield 30%. ^{1}H NMR ($CDCl_3$): δ 7.45−7.20 (m, 5H), 7.20−7.00 (m, 6H), 4.93−4.69 (m, 2H), 4.10−4.00 (m, 6H), 3.80−3.70 (m, 2H), 3.60−2.85 (m, 16H), 2.36 (s, 3H), 2.31 (s, 6H), 2.10−1.95 (m, 4H), 1.55−1.48 (m, 4H), 1.35 (s, 9H), 1.25 (s, 9H), 1.15 (s, 9H), 0.90−0.75 (m, 6H). ^{13}C NMR ($CDCl_3$): δ 172.3, 167.9, 167.1, 151.9, 151.3, 136.5−126.6, 81.5, 80.9, 70.6, 70.4, 69.6, 68.56, 67.6, 48.4, 46.3, 31.9, 27.9, 21.0, 20.7, 19.3, 13.9. Mass spectrum (FAB): m/z = 1053.5 [(M + H)$^+$, calcd for $C_{62}H_{89}N_2O_{12}$ 1053.6].

Triphenylene-Functionalized Triester (7). A solution of triphenylene-2-carboxylic acid **3** (0.10 g, 0.37 mmol) in $SOCl_2$ (10 mL) was refluxed for 4 h. Subsequently, the excess $SOCl_2$ was removed in vacuo. The acid chloride **4** was redissolved in CH_2Cl_2 (5 mL) and added to a solution of mono(amide) **6** (0.30 g, 0.29 mmol) and Et_3N (0.10 g, 1.0 mmol) in CH_2Cl_2 (100 mL). The resulting solution was stirred overnight at room temperature. Subsequently CH_2Cl_2 was added (100 mL) and the reaction mixture was washed twice with 1 N HCl, followed by standard workup. The crude product was purified by flash column chromatography (ethyl acetate/hexane, 2:3) to give **7** as a white solid, yield 60%. Mp: 61−63 °C. ^{1}H NMR ($CDCl_3$): δ 8.86−8.60 (m, 6H), 8,29 (d, 1H, J = 8.0 Hz), 7.80−6.90 (m, 15H), 5.15 (s, 2H), 5.03 (s, 2H), 4.93 (s, 2H), 4.77 (s, 2H), 4.25−3.04 (m, 18H), 2.40−1.80 (m, 17H), 1.68−0.80 (m, 37H). ^{13}C NMR ($CDCl_3$): δ 172.3, 167.9, 167.1, 151.9, 151.3, 136.5−123.4, 81.5, 80.9, 70.6, 70.4, 69.6, 68.56, 67.6, 48.4, 46.3, 31.9, 27.9, 21.0, 20.7, 19.3, 13.9. Mass spectrum (FAB): m/z = 1330.3 [(M + Na)$^+$, calcd 1329.7]. Anal. Calcd. for $C_{81}H_{98}N_2O_{13}$: C, 74.40; H, 7.55; N, 2.14. Found: C, 74.15; H, 7.48; N, 2.20.

Triphenylene-Functionalized Triacid (H_3)1. A solution of triester **7** (0.20 g, 0.18 mmol) in TFA (15 mL) was stirred overnight at room temperature. Subsequently, toluene (15 mL) was added, and the TFA/toluene mixture was azeotropically evaporated. The residue was taken up in CH_2Cl_2 (100 mL) and washed twice with 1 N HCl, followed by standard workup. The triacid (H_3)**1** was obtained as a white solid in quantitative yield. Mp: 102−104 °C. ^{1}H NMR (MeOD-d_4): δ 8.80−8.10 (m, 7H), 7.70−6.80 (m, 15H), 5.10−4.60 (m, 4H), 4.20−4.90 (m, 18H), 2.35−2.15 (m, 9H), 2.10−0.70 (m, 18H). Mass spectrum (FAB): m/z = 1161.4 [(M + Na)$^+$, calcd 1161.5]. Anal. Calcd for $C_{69}H_{74}N_2O_{13}\cdot H_2O$: C, 71.61; H, 6.62; N, 2.42. Found: C, 71.39; H, 6.50; N, 2.40.

General Procedure for the Preparation of the Complexes. To a solution of 1.0 equiv of triacid (H_3)**1** and 4.0 equiv of Et_3N in methanol was added 1.1 equiv of the lanthanide nitrate salt. The resulting solution was stirred for 2 h, after which the solvent was concentrated to dryness in vacuo. The complex was redissolved in $CHCl_3$ and washed twice with water, followed by standard workup. The complexes were obtained as solids in quantitative yields. The complexes were characterized by FAB mass spectrometry and IR spectroscopy. FAB-MS data: [(Eu)**1**]: m/z = 1289.3 [(M + H)$^+$, calcd 1289.4]; [(Tb)**1**] m/z = 1295.2 [(M + H)$^+$, calcd 1295.4]; [(Gd)**1**] m/z = 1294.1 [(M + H)$^+$, calcd 1294.4]; [(Er)1] m/z = 1304.5 (M + H)$^+$, calcd 1304.4]; [(Yb)**1**] m/z = 1310.4 [(M + H)$^+$, calcd 1310.4]; [(Nd)**1**]: m/z = 1280.3 [(M + H)$^+$, calcd 1280.4]. The complexes all gave similar IR spectra: a peak at 1635−1630 cm^{-1} ($\nu_{NC=O}$) with a shoulder around 1600−1590 cm^{-1} (ν_{COO}).

Photophysical Studies. Steady-state luminescence measurements in the visible region were performed with a Photon Technology International (PTI) Alphascan spectrofluorimeter, which has a 75 W quartz−tungsten−halogen lamp as the excitation source and a Hamamatsu R928 photomultiplier. For steady-state photoluminescence measurements in the near-IR region, the excitation light beam was modulated with a mechanical chopper at 40 Hz. The luminescence signal was detected with a liquid nitrogen cooled Ge detector, using standard lock-in techniques. Alternatively, the 351.1/363.8 nm lines of an Ar ion pump laser at a power of 60 mW were used for excitation. The laser beam was modulated with an acoustooptic modulator at a frequency of 40 Hz.

Time-resolved luminescence measurements in the visible region were performed with an Edinburgh Analytical Instruments FL900 system. Luminescence lifetime measurements (Edinburgh Analytical Instruments LP900 system) in the near-IR-region were performed by monitoring the luminescence decay after excitation with a 0.5 ns pulse of a LTB MSG 400 nitrogen laser (λ_{exc} = 337 nm, pulse energy 20 μJ, 10 Hz repetition rate). Decay signals were recorded using a liquid nitrogen cooled Ge detector with a time resolution of 0.3 μs. The signals were averaged using a digitizing Tektronix oscilloscope. All decay curves were analyzed by deconvolution of the measured detector response and fitting with monoexponential functions.

The quantum yield of the triphenylene fluorescence and the quantum yield of the overall sensitized lanthanide emission were determined relative to a reference solution of quinine sulfate in 1 M H_2SO_4 (ϕ = 0.546), and correctected for the refractive index of the solvent.[53] The absorbance of the solutions was 0.1 at the excitation wavelength (310 nm). The solvents were of spectroscopic grade. Deaeration of the samples was performed by purging the solutions thoroughly with Ar(g) for15−20 min.

Transient Absorption Spectroscopy. The 340 nm pump light was delivered by a frequency-doubled tunable optical parametric oscillator system (Coherent Infinity XPO). The width of the pulse was approximately 2 ns (fwhm), and its energy was less than 1 mJ/pulse. For recording the transient absorption spectra at a definite time after the laser pulse, the probe light from a flashlamp (EG&G FX504, 2.5 μs pulse width) went via the sample through a spectrograph (Acton SpectraPro 150) to a gated intensified charge-coupled device camera (Princeton Instruments ICC-576-G/RB-EM). This system was also used to obtain kinetic data in the microsecond domain by recording a set of transient spectra at increasing time intervals. Alternatively, the flashlamp was used in combination with the streak camera system (Hamamatsu) as the detector to simultaneously probe the wavelength and time dependence of the transient signals in the submicrosecond domain. The streak images

containing the transient absorbance data were subjected to principal component analysis by means of singular value decomposition. All the datasets contained only one significant component. This component was used in the reconstruction of the transient absorption spectrum of this single component in the top of the excitation pulse and its kinetics.

Electrochemical Measurements. Cyclic voltammetry was performed in a three-electrode cell containing a platinum working electrode, a platinum counter electrode, and a Ag/AgCl reference electrode, with an Autolab PGSTAT10 (ECO-CHEMIE, Utrecht, The Netherlands). The ferrocene/ferricinium redox couple was used as an internal standard ($E° = 0.44$ V vs SCE in DMSO).[54] The solvent DMSO was of spectroscopic grade and was deoxygenated by being purged with nitrogen. The ground electrolyte was Bu_4NPF_6 (0.1 M). The measurements were performed in a glovebox under a nitrogen atmosphere. The cyclic voltammograms were recorded at a scan rate of 100 mV/s.

Acknowledgment. Akzo Nobel Research is gratefully acknowledged for its financial and technical support. Frank Steemers (University of Twente) is gratefully acknowledged for his contribution to the synthesis of the triphenylene antenna. Lenneke Slooff and Professor Albert Polman (FOM Institute for Atomic and Molecular Physics, The Netherlands) are gratefully acknowledged for their support with the near-infrared luminescence measurements. We express gratitude to Professor Jan Verhoeven (University of Amsterdam) for his valuable comments. This research has been financially supported by the Council for Chemical Sciences of The Netherlands Organization for Scientific Research (CW-NWO).

References and Notes

(1) Mukkala, V.-M.; Helenius, M.; Hemmilä, I.; Kankare, J.; Takalo, H. *Helv. Chim. Acta* **1993**, *76*, 1361.

(2) Slooff, L. H.; Polman, A.; Oude Wolbers, M. P.; van Veggel, F. C. J. M.; Reinhoudt, D. N.; Hofstraat, J. W. *J. Appl. Phys.* **1997**, *83*, 497.

(3) Oude Wolbers, M. P.; van Veggel, F. C. J. M.; Peters, F. G. A.; van Beelen, E. S. E.; Hofstraat, J. W.; Geurts, F. A. J.; Reinhoudt, D. N. *Chem. Eur. J.* **1998**, *4*, 772.

(4) (a) Gschneider, K. A.; Eyring, L. R. *Handbook on the Physics and Chemistry of Rare Earths*; North-Holland Publishing Co.: Amsterdam, 1979. (b) Sabbatini, N.; Guardigli, M.; Lehn, J.-M. *Coord. Chem. Rev.* **1993**, *123*, 201 and references therein.

(5) Sato, S.; Wada, M. *Bull. Chem. Soc. Jpn.* **1970**, *43*, 1955.

(6) Crosby, G. A.; Whan, R. E.; Alire, R. M. *J. Chem. Phys.* **1961**, *34*, 743.

(7) Tanaka, M.; Yamagughi, G.; Shiokawa, J.; Yamanaka, C. *Bull. Chem. Soc. Jpn.* **1970**, *43*, 549.

(8) Haynes, A. V.; Drickamer, H. G. *J. Chem. Phys.* **1982**, *76*, 114.

(9) (a) Tobita, S.; Arakawa, M.; Tanaka, I. *J. Phys. Chem.* **1984**, *88*, 2697. (b) Tobita, S.; Arakawa, M.; Tanaka, I. *J. Phys. Chem.* **1985**, *89*, 5649.

(10) Dexter, D. L. *J. Chem. Phys.* **1953**, *21*, 836.

(11) Sabbatini, N.; Guardigli, M.; Manet, I.; Ungaro, R.; Casnati, A.; Ziessel, R.; Ulrich, G.; Asfari, Z.; Lehn, J.-M. *Pure Appl. Chem.* **1995**, *67*, 135.

(12) Parker, D.; Williams, J. A. G. *J. Chem. Soc., Dalton Trans.* **1996**, 3613, and references therein.

(13) (a) Oude Wolbers, M. P.; van Veggel, F. C. J. M.; Snellink-Ruël, B. H. M.; Hofstraat, J. W.; Geurts, F. A. J.; Reinhoudt, D. N. *J. Am. Chem. Soc.* **1997**, *119*, 138. (b) Oude Wolbers, M. P.; van Veggel, F. C. J. M.; Hofstraat, J. W.; Geurts, F. A. J.; Reinhoudt, D. N. *J. Chem. Soc., Perkin Trans. 2* **1997**, 2275. (c) Oude Wolbers, M. P.; van Veggel, F. C. J. M.; Snellink-Ruël, B. H. M.; Hofstraat, J. W.; Geurts, F. A. J.; Reinhoudt, D. N. *J. Chem. Soc., Perkin Trans. 2* **1998**, 2141.

(14) Rudkevich, D. M.; Verboom, W.; van der Tol, E. B.; van Staveren, C.; Kaspersen, F.; Verhoeven, J. W.; Reinhoudt, D. N. *J. Chem. Soc., Perkin Trans. 2* **1995**, 131.

(15) Hemmilä, I. K. *Applications of Fluorescence in Immunoassays*; Wiley and Sons: New York, 1991.

(16) Werts, M. H. V.; Hofstraat, J. W.; Geurts, F. A. J.; Verhoeven, J. W. *Chem. Phys. Lett.* **1997**, *276*, 196.

(17) Heller, A. *J. Am. Chem. Soc.* **1967**, *89*, 167.

(18) Iwamuro, M.; Hasegawa, Y.; Wada, Y.; Murakoshi, K.; Kitamura, T.; Nakashima, N.; Yamanaka, T.; Yanagida, S. *Chem. Lett.* **1997**, 1067.

(19) Desurvire, E. *Phys. Today* **1994**, *97*, 20.

(20) Oshishi, Y.; Kanamori, T.; Kitagawa, T.; Takashashi, S.; Snitzer, E.; Sigel Jr., G. H. *Opt. Lett.* **1991**, *16*, 1747.

(21) An, D.; Yue, Z.; Chen, R. T. *Appl. Phys. Lett.* **1998,** *72*, 2806.

(22) Steemers, F. J.; Verboom, W.; Reinhoudt, D. N.; van der Tol, E. B.; Verhoeven, J. W. *J. Am. Chem. Soc.* **1995**, *117*, 9408.

(23) Murov, S. L.; Carmichael, I.; Hug, G. L. *Handbook of Photochemistry*, 2nd ed.; Marcel Dekker Inc.: New York, 1993.

(24) Klink, S. I.; Hebbink, G. A.; Grave, L.; Peters, F. G. A.; Van Veggel, F. C. J. M.; Reinhoudt, D. N.; Hofstraat, J. W. *Eur. J. Org. Chem.*, in press.

(25) Klink,S. I.; Hebbink, G. A.; Grave, L.; van Veggel, F. C. J. M.; Reinhoudt, D. N.; Slooff, L. H.; Polman, A.; Hofstraat, J. W. *J. Appl. Phys.* **1999**, *86*, 1181.

(26) Jorgenson, W. L.; Briggs, J. M. *Mol. Phys.* **1988**, *63*, 547.

(27) van Veggel, F. J. C. M.; Reinhoudt, D. N. *Recl. Trav. Chim. Pays-Bas* **1995**, *114*, 387. The Lennard-Jones parameters for the Ln^{3+} ions were taken from: van Veggel, F. C. J. M.; Reinhoudt, D. N. *Chem. Eur. J.* **1999**, *5*, 90.

(28) (a) Kirby, A. F.; Foster, D.; Richardson, F. S. *Chem. Phys. Lett.* **1983**, *95*, 507. (b) Kirby, A. F. Richardson, F. S. *J. Phys. Chem.* **1983**, *87*, 2544.

(29) ^{1}H NMR spectra of similar complexes in DMSO-d_6 show that these types of complexes have a (time-averaged) C_s symmetry. See also ref 24.

(30) Richardson, F. S. *Chem. Rev.* **1982**, *82*, 541.

(31) (a) Kropp, J. L.; Windsor, M. W. *J. Chem. Phys.* **1963**, *39*, 2769. (b) Kropp, J. L.; Windsor, M. W. *J. Chem. Phys.* **1965**, *42*, 1599. (c) Kropp, J. L.; Windsor, M. W. *J. Chem. Phys.* **1966**, *45*, 761.

(32) (a) Horrocks, W. D., Jr.; Sudnick, D. R. *Acc. Chem. Res.* **1981**, *14*, 384. (b) Holz, R. C.; Chang, C. A.; Horrocks, W. D., Jr. *Inorg. Chem.* **1991**, *30*, 3270.

(33) Beeby, A.; Clarkson, J. M.; Dickins, R. S.; Faulkner, S.; Parker, D.; Royle, L.; de Sousa, A. S.; Williams, J. A. G.; Woods, M. *J. Chem. Soc., Perkin Trans. 2* **1999**, 493.

(34) Frey, S. T.; Horrocks,W. D., Jr. *Inorg. Chim. Acta* **1995**, *229*, 383 and references therein.

(35) (a) Hasegawa, Y.; Kimura, Y.; Murakoshi, K.; Wada, Y.; Kim, J.-H.; Nakashima, N.; Yamanaka, T.; Yanagida, S. *J. Phys. Chem.* **1996**, *100*, 10201. (b) Hasegawa, Y.; Murakoshi, K.; Wada, Y.; Yanagida, S.; Kim, J.-H.; Nakashima, N.; Yamanaka, T. *Chem. Phys. Lett.* **1996**, *248*, 8.

(36) (a) Carnall, W. T.; Goodman, G. L.; Rajnak, K.; Rana, R. S. *J. Chem. Phys.* **1989**, *90*, 3443. (b) Beeby, A.; Dickins, R.; Faulkner, S.; Parker, D.; Williams, J. A. G. *J. Chem. Soc., Chem. Commun.* **1997**, 1401.

(37) Steemers, F. J.; Verboom, W.; Hofstraat, J. W.; Geurts, F. A. J.; Reinhoudt, D. N. *Tetrahedron Lett.* **1998**, *39*, 7583.

(38) Crosby, G. A.; Kasha, M. *Spectrochim. Acta* **1958**, *10*, 377.

(39) Stein, G.; Würzberg, E. *J. Chem. Phys.* **1975**, *62*, 208.

(40) Weber, M. J. *Phys. Rev.* **1968**, *171*, 283.

(41) (a) Sabbatini, N.; Perathoner, S.; Lattanzi, G.; Dellonte, S.; Balzani, V. *J. Phys. Chem.* **1987**, *91*, 6136. (b) Steemers, F. J.; Meuris, H. G.; Verboom, W.; Reinhoudt, D. N. *J. Org. Chem.* **1997**, *62*, 4229.

(42) The reduction potential of Eu^{3+} is -0.35 V in water (vs NHE). Bard, A. J.; Parsons, R.; Jordan, J. *Standard Potentials in Aqueous Solution*; Marcel Dekker Inc.: New York, 1985.

(43) k_{diff} is taken as 10^{10} s^{-1}; $[O_2]$ in methanol is 2.1 mM (ref 23). Since $k_{ox} = k_{diff}[O_2] = 2 \times 10^7$ s^{-1}, and there is no oxygen effect, $k_{ET} > k_{ox}$, which means that k_{ET} exceeds 10^7 s^{-1}.

(44) Bhaumik, M. L.; El-Sayed. *J. Chem. Phys.* **1965**, *42*, 787.

(45) Bhattacharyya, S.; Sousa, L. R.; Ghosh, S. *Chem. Phys. Lett.* **1998**, *297*, 154.

(46) $\phi_{se} = \phi_{isc}\phi_{et}\phi_{lum} = \phi_{isc}\phi_{et}\tau/\tau_0$. Typical values of the natural lifetime τ_0 of Eu^{3+} and Tb^{3+} are 3 and 4 ms, respectively. If ϕ_{isc} and ϕ_{et} are taken as 1, then based on the luminescence lifetimes ϕ_{se} is 0.29 for (Eu)**1** and 0.44 for (Tb)**1**.

(47) It can be demonstrated that a photon-induced electron-transfer process may indeed be the additional cause of the low luminescence quantum yield of (Eu)**1**. The antenna fluoresence lifetime of (Tb)**1** was measured to be approximately 1 ns. Using the equation $\phi_{flu} = k_{flu}/(k_{flu} + k_{isc}) = k_{flu}\tau_{flu}$, it follows that $k_{flu} = 0.86 \times 10^7$ s^{-1} and $k_{isc} = 9.9 \times 10^8$ s^{-1}. It can furthermore be calculated that $\phi_{isc} \gg 0.99$. If it is assumed that k_{flu} and k_{isc} are the same for (Eu)**1** as for (Tb)**1**, then the rate of the photon-induced electron transfer (k_{PET}) can be calculated via $\phi_{flu} = k_{flu}/(k_{flu} + k_{isc} + k_{PET})$, resulting in $k_{PET} = 5.9 \times 10^8$ s^{-1}. As a result, the intersystem crossing yield of (Eu)**1** is lower than that of (Tb)**1** with $\phi_{isc} \approx 0.63$.

(48) Van der Tol, E. B. *Design and Photophysics of Luminescent Labels for Use in Time-Resolved Biological Assays*. Ph.D. Thesis, University of Amsterdam, 1998.

(49) Horrocks, W. D., Jr.; Bolender, J. P.; Smith, W. D.; Supkowski, R. M. *J. Am. Chem. Soc.* **1997**, *119*, 5972 and references therein.

(50) The reduction potential of Yb^{3+} in water is −1.05 V (vs NHE). See ref 42.
(51) This complex has a phenyl group instead of a triphenylene moiety. See ref 24.
(52) Pysh, E. S.; Yang, N. C. *J. Am. Chem. Soc.* **1963**, *85*, 2124.
(53) Demas, N. J.; Crosby, G. A. *J. Phys. Chem.* **1971**, *75*, 991.
(54) Barrette, W. C., Jr.; Johnson, H. W., Jr.; Sawyer, D. T. *Anal. Chem.* **1984**, *56*, 1890.